IEEE Access
Multidisciplinary | Rapid Review | Open Access Journal

Received April 22, 2018, accepted May 19, 2018, date of publication May 25, 2018, date of current version June 26, 2018.

Digital Object Identifier 10.1109/ACCESS.2018.2840538

Sliding Mode Tracking Control With Perturbation Estimation for Hysteresis Nonlinearity of Piezo-Actuated Stages

RUI XU[1], XIUYU ZHANG[2], (Member, IEEE), HONGYAN GUO[1], (Member, IEEE), AND MIAOLEI ZHOU[1], (Member, IEEE)

[1]Department of Control Science and Engineering, Jilin University, Changchun 130012, China
[2]School of Automation Engineering, Northeast Dianli University, Jilin City 132012, China

Corresponding author: Miaolei Zhou (zml@jlu.edu.cn)

This work was supported in part by the National Natural Science Foundation of China under Grant 51675228, in part by the Fundamental Research Funds for the Central Universities under Grant 451170301194, and in part by the Program of Science and Technology Development Plan of Jilin Province of China under Grant 20180101052JC.

ABSTRACT Piezo-actuated stages are widely applied in the field of high-precision positioning. However, piezo-actuated stages produce hysteresis between the input voltage and the output displacement that negatively influences the positioning accuracy. In this paper, the Bouc–Wen model is established and identified using the bat-inspired optimization algorithm. Subsequently, based on the established hysteresis model, we propose a sliding mode control method with a new reaching law to suppress the hysteresis nonlinearity and achieve high-precision tracking control for the piezo-actuated stages. In addition, the proposed control method contains the perturbation estimation part, which can estimate online the modeling uncertainty and the unknown external disturbances. The stability of the proposed control method is demonstrated through the Lyapunov theory. Finally, to validate the effectiveness of the proposed control method, experiments are conducted on the piezo-actuated stages. Experimental results demonstrate that the proposed control method is superior to the feed-forward control and the conventional sliding mode control method.

INDEX TERMS Sliding mode tracking control, piezo-actuated stages, hysteresis, Bouc–Wen model.

I. INTRODUCTION

Micro/nano positioning stages driven by the piezoceramic actuators are widely applied in ultrahigh precision systems, such as a lithography machine, ultra-precision turning machine, scanning probe microscope, astronomical telescope, and biological manipulation [1]–[3]. This is because piezoceramic actuators have the advantages of high stiffness, minimal heat generation, and large blocking force [4], [5]. However, the primary weakness of the piezo-actuated stages is the severe hysteresis nonlinearity between the input voltage and the output displacement. The hysteresis effect has the characteristics of consistency and non-memoryless, that can severely affect tracking precision and response speed [6], [7]. The most effective method to eliminate the hysteresis effect of the piezo-actuated stages is to adopt an appropriate control strategy. In the design of the control method, the modeling of piezo-actuated stages has attracted considerable attention, and certain hysteresis models have been established to describe the hysteresis nonlinearity, such as Preisach model [8], Prandtl-Ishlinskii model [9], Krasnosel'skii-Pokrovskii (KP) model [10], Bouc-Wen model [11], and Maxwell model [12].

The feed-forward control method based on the inverse hysteresis model is commonly used to address the hysteresis effect in the piezo-actuated stages. For instance, a compensator based on an inverse Bouc-Wen model was used to design a feed-forward controller [13]. This proposed control method drew considerable attention in terms of a simplified implementation. To ensure precision, the hybrid control method composed of feed-forward and feedback control is extensively applied in the piezo-actuated stages [14]. The proportional-integral-derivative (PID) control is a common control method to suppress the hysteresis effect in the piezo-actuated stages at low frequencies. For instance, the feed-forward control integrated with a proportional-integral (PI) control was proposed [15]. The PI control can effectively reduce the steady-state error and improve the tracking precision of the piezo-actuated stages. However, the standard

2169-3536 © 2018 IEEE. Translations and content mining are permitted for academic research only.
Personal use is also permitted, but republication/redistribution requires IEEE permission.
See http://www.ieee.org/publications_standards/publications/rights/index.html for more information.

PID control has poor resistance for external disturbances and model uncertainty. Hence, a series of robust control strategies are designed to achieve the high-precision tracking control of the piezo-actuated stages. The feed-forward control combined with a robust controller was designed to improve the tracking precision [16]. A H_∞ robust controller with an inverse compensator was introduced to achieve real-time tracking control of giant magnetostrictive actuators [17]. However, the feed-forward control based on the inverse hysteresis is a particularly complicated method, that requires numerous mathematical operations and increases the controller design difficulty.

The conventional sliding mode control (CSMC) is a classical nonlinear control method that can solve the hysteresis nonlinearity problem effectively [18], [19]. The structure of the CSMC system varies with the current state of the system, and drives the system's states on the scheduled sliding mode surface within the restricted time. The design of the sliding mode control can be divided into two parts: the design of the sliding surface and the design of feedback control law. According to [20], the CSMC method with an integral sliding surface exhibits a better performance than the traditional proportional one. In this study, we adopt the integral sliding surface to describe the dynamic property of the SMC method. The feedback control law of the SMC method is designed using the reaching law, which can accelerate the convergence rate of the sliding surface. Furthermore, the CSMC has the characteristics of robustness and exceptional tracking performance with regard to the piezo-actuated stages with external disturbances, and the hysteresis can be considered as the uncertainty or interference factor. However, the prior knowledge of the hysteresis is necessary, which can influence the control performance of the CSMC for the piezo-actuated stages. To address this problem, a sliding mode control with perturbation estimation (SMCPE) was designed [21]–[23], where the modeling uncertainties were replaced using the method of online estimation for the perturbations. Moreover, the chattering problem deteriorates the performance of the sliding mode controller. The boundary layer approach is used to reduce the chattering of the control systems [24]. In addition, the boundary layer with the sigmoid function was designed to eliminate the chattering with regard to the SMC method. Experimental results indicated that the proposed SMC method suppressed the hysteresis effect in the piezo-actuated stages [25]. Designing high-order SMC is also a technique to solve the chattering problem. To remove the chattering of the SMC method, Xu proposed a third-order sliding mode motion control for the piezo-actuated stages; experimental results confirmed that the proposed control method realized the high precision tracking control of the piezo-actuated stages [26].

In this study, a sliding mode control method is proposed, which introduces the PI-type sliding surface and a new reaching law composed of the power reaching law and the constant reaching law. The new reaching law has been attained by combining the advantages of the power reaching law and the constant reaching law. When the sliding surface is large, the power reaching law plays a major role in the sliding mode control; when the sliding surface is small, the constant reaching law plays a major role in the sliding mode control. Therefore, the new reaching law enhances the performance of the proposed controller. Moreover, the stability of the proposed control method is analyzed using the Lyapunov theory. Subsequently, to demonstrate the tracking performance of the proposed control method, experiments with regard to the piezo-actuated stages are conducted. The experimental results indicate that the proposed control method demonstrates the best tracking performance in comparison with the feed-forward control and the CSMC method.

The primary contributions of this study are summarized as follows: 1) The bat-inspired algorithm is firstly adopted to identify the unknown parameters of the Bouc-Wen model, and the identification model can describe the major and minor hysteresis loops of the piezo-actuated stages. 2) A perturbation estimation method is employed to estimate the modeling uncertainty and the unknown external disturbances. 3) To suppress the hysteresis nonlinearity of the piezo-actuated stages, a new reaching law is proposed to design the proposed control method. The effectiveness of the proposed control method is verified on the experimental setup. 4) The stability of the proposed control method is analyzed using the Lyapunov stability theory.

The remainder of this paper is organized as follow. A Bouc-Wen model is established and the unknown parameters are identified by the bat-inspired optimization algorithm in section II. Then, section III introduces a CSMC method based on the Bouc-Wen model to achieve the high-precision tracking of the piezo-actuated stages. Considering the external perturbation and the modeling uncertainty, a sliding mode tracking control with perturbation estimation is proposed and the stability analysis is proved by the Lyapunov theory. In section IV, compared with the feed-forward control and the CSMC method, the efficiency of the proposed controller is demonstrated by the experimental results. Finally, section V gives the conclusion.

II. DESCRIPTION AND IDENTIFICATION OF THE BOUC-WEN MODEL

A. BOUC-WEN MODEL

The generalized Bouc-Wen model was proposed by Bouc in 1967 [27]. Wen [28] expanded this model, which can describe a large class of hysteresis nonlinearity systems in the form of differential equations. In this study, the Bouc-Wen model is used to describe the piezo-actuated stages system, which is expressed as

$$\begin{cases} \dot{x} = a_0 x + a_1 u + a_2 w + f \\ \dot{w} = \alpha \dot{u} - \beta \left|\dot{u}\right| w|w|^{n-1} - \gamma \dot{w}|w|^n \\ y = x, \end{cases} \tag{1}$$

where x is the system state, u and y denote the input voltage and the output displacement of the piezo-actuated stages

respectively. a_0, a_1, and a_2 are the nominal parameters of the system. w is the hysteresis term of the Bouc-Wen model, the coefficients α, β, and γ determine the amplitude and shape of the Bouc-Wen model respectively, the coefficient n influences the smoothness of the transition from elastic to plastic responses, f represents the unknown external perturbation of the system.

B. MODEL IDENTIFICATION BASED ON BAT-INSPIRED OPTIMIZATION ALGORITHM

Owing to the complexity of the Bouc-Wen model, it is difficult to identify the unknown parameters of the model using the conventional method [29], [30]. In this study, the bat-inspired optimization algorithm is used for the first time to identify the seven unknown parameters. The bat-inspired optimization algorithm is a new intelligent optimization algorithm introduced by Yang [31] in 2010, which is inspired by the bat echo fixed position. Compared with the other optimization algorithms, the bat-inspired algorithm has faster convergent rate and stronger robustness, which is widely used to address the high-dimensional nonlinear problem [32], [33]. To facilitate the identification of the unknown parameters of the Bouc-Wen model, Eq.(1) is rewritten using the discrete form of the state-space model as [30]

$$Y_{\mathrm{b}}(k+1) = F\left(k, Y_{\mathrm{b}}(k), u(k), \Theta\right), \tag{2}$$

where $u(k)$ is the input voltage, $\Theta = (a_0, a_1, a_2, \alpha, \beta, \gamma, n)$ is the unknown parameter of the piezo-actuated stages system based on Bouc-Wen model, $Y_{\mathrm{b}} \in R^q$ are the state vector, which represents the output displacement of the system based on Bouc-Wen model.

To identify the parameters of the Bouc-Wen model accurately, an appropriate fitness function requires to be designed. In this study, the fitness function described by the mean-square error is selected as follows

$$J_{\mathrm{mse}} = \frac{1}{N}\sum_{i=1}^{N}\left(Y^i_{\mathrm{actual}}(t) - Y^i_{\mathrm{b}}(t)\right)^2, \tag{3}$$

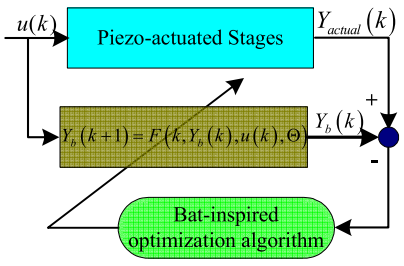

FIGURE 1. Block diagram of parameter identification process.

where Y^i_{actual} and Y^i_{b} represent the experimental output data of the piezo-actuated stages and the output data of the Bouc-Wen model at the tth sampling time, respectively. N is the total number of the output data. The block diagram of the identification process is shown in Fig. 1. Evidently, the process of parameter identification can be regarded as a numerical optimization problem, where the variable is the unknown parameter Θ, and the bat-inspired optimization algorithm is used to adjust the parameters of the system model. The identification principle of the system based on Bouc-Wen model is defined as follows

$$\min J_{\mathrm{mse}} \quad \text{subject to} \begin{cases} \dot{x} = & a_0 x + a_1 u + a_2 w + f \\ \dot{w} = & \alpha\dot{u} - \beta\,|\dot{u}|\,w|w|^{n-1} - \gamma\dot{w}|w|^n \end{cases} \tag{4}$$

In the process of model identification based on the bat-inspired algorithm, the unknown parameters satisfy $\Theta_L \le \Theta \le \Theta_H$; Θ_L and Θ_H are the lower and upper bound of the unknown parameters.

During the operation of the optimization algorithm, the velocity and position of each bat are updated with regard to the changes in the frequency. The velocities v_i^t and position x_i^t are updated using the following equations

$$f_i = f_{\min} + (f_{\max} - f_{\min})\,\beta, \tag{5}$$

$$v_i^t = v_i^{t-1} + \left(x_i^{t-1} - x_*^t\right) f_i, \tag{6}$$

$$x_i^t = x_i^{t-1} + v_i^t, \tag{7}$$

where $f_i \in [f_{\min}, f_{\max}]$ is the fixed frequency of the individual bat. β is a random number and $0 \le \beta \le 1$, x_* is the current global optimum, which is compared with all the solutions among all the n bats at each iteration t.

To improve the diversity of the optimization algorithm, a new solution of each bat is deduced using Eq.(8).

$$x_{\mathrm{new}} = x_{\mathrm{old}} + \zeta A^t, \tag{8}$$

where $\zeta \in [-1, 1]$ is a random number. A^t is the average loudness of all bats at time-step t.

At beginning of the algorithm operation process, the bat has an exceedingly small pulse rate and a larger loudness. It has a larger probability to select a better solution. With the increasing iterations, the bat scans for prey to solve the best solution using the increasing pulse rate and the decreasing loudness. The loudness A_i and the pulse rate r_i are updated by Eq.(9) and Eq.(10).

$$A_i^{t+1} = \kappa A_i^t, \tag{9}$$

$$r_i^{t+1} = r_i^0\left[1 - \exp\left(-\delta t\right)\right], \tag{10}$$

where κ and δ are constants, respectively. r_i^0 is the initial pulse rate.

The procedure of the Bouc-Wen model identification is as follows

(i) Collecting the experiment data: a range of 0-90 V triangular wave voltage signal (with frequency 1 Hz) is exerted on the piezo-actuated stages; the output displacement of the piezo-actuated stages is measured and saved.

(ii) Identification of the Bouc-Wen model: when the bat-inspired optimization algorithm is running,

the unknown parameter Θ is replaced by the position of the bat. With the program operating based on the identification principle of the Bouc-Wen model, the unknown parameters Θ of the Bouc-Wen model is identified.

(iii) Model measurements: the Bouc-Wen model based on the bat-inspired optimization algorithm is applied in the MATLAB/Simulink software.

TABLE 1. Identified model parameters.

Parameters	Value	Units
a_0	-1550.36	-
a_1	1939.74	-
a_3	-1643.57	-
α	0.4214	μm/V
β	0.6523	V^{-1}
γ	0.2489	V^{-1}
n	1.2	-

The parameters of the obtained model based on the bat-inspired optimization algorithm are described in Table 1, and hysteresis loop of the obtained model is shown in Fig. 2(a). It is evident that this hysteresis loop is generally consistent with the data obtained from the piezo-actuated stages. In addition, the prediction errors of the obtained model are shown in Fig. 2(b), and it can be observed that the maximum (MAX) error is 0.9651 μm, which is 2.59% of the MAX displacement of the piezo-actuated stages. In view of the uncertain parameters, the piezo-actuated stages system based on Bouc-Wen model is described as

$$\begin{cases} \dot{x} = (a_0 + \Delta_0)x + (a_1 + \Delta_1)u + (a_2 + \Delta_2)w + f \\ \dot{w} = \alpha\dot{u} - \beta\,|\dot{u}|\,w|w|^{n-1} - \gamma\dot{w}|w|^n \\ y = x, \end{cases} \tag{11}$$

where Δ_0, Δ_1, and Δ_2 are the uncertain parameters part, $\Phi = \Delta_0 x + \Delta_1 u + \Delta_2 w + f$ includes the total disturbance caused by the external noise, uncertain parameters, which is assumed to be bounded and reduced using the sliding mode control method.

III. SLIDING MODE CONTROLLER DESIGN

A. CSMC METHOD DESIGN

A CSMC method is designed based on the established system model (i.e. Eq.(2)) in the study. To design the CSMC, a tracking error is defined as follows

$$e(t) = x_d(t) - x(t), \tag{12}$$

where $x_d(t)$ and $x(t)$ represent the desired displacement and the actual output displacement of the piezo-actuated stages, respectively. $e(t)$ is the error between $x_d(t)$ and $x(t)$. According to Eq.(1), the PI-type sliding surface function is defined as follows

$$s(t) = e(t) + \lambda \int_0^t e(\tau)\,d\tau, \tag{13}$$

where λ is a positive constant, which is adjusted according to the performance of the controller.

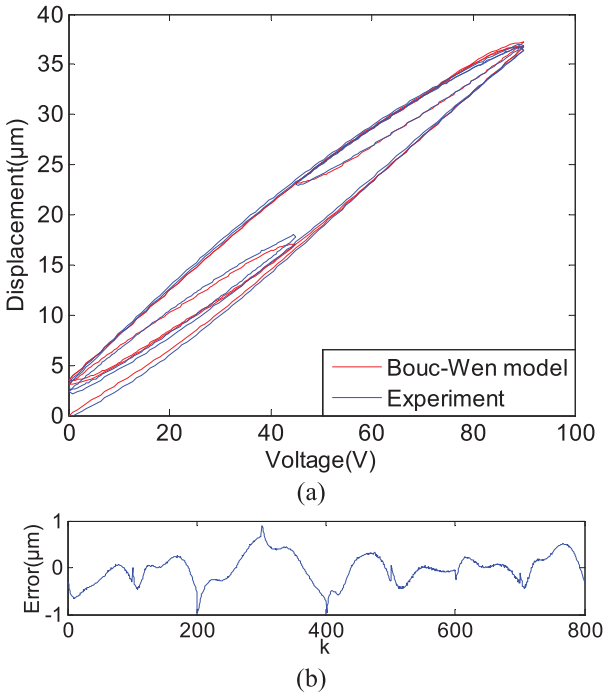

FIGURE 2. Results of identified Bouc-Wen model. (a) Comparison of Bouc-Wen model and experimental result. (b) Prediction errors of identified Bouc-Wen model.

Combined with Eq.(13) and Eq.(1), the control law is designed as follows

$$u = \frac{1}{a_1}(\dot{x}_d - a_0 x + k_s|s|^{\varepsilon}\mathrm{sgn}(s) - a_2 w + \lambda e), \tag{14}$$

where sgn$(\cdot)$ denotes the signum function, and $k_s \in \Re^+$ and ε are the positive constants.

Theorem: For the piezo-actuated stage system (i.e. Eq.(1)) with the Φ, the control law (i.e. Eq.(14)) is obtained; when the $t \to \infty$, the sliding mode surface satisfies that

$$|s(t)| \le \left(\frac{\Phi}{k_s}\right)^{\frac{1}{\varepsilon}} \tag{15}$$

Proof: With regard to the effectiveness and stability of the designed sliding mode controller, the Lyapunov function is defined as follows

$$V = \frac{1}{2}s^2. \tag{16}$$

By taking the time derivative of Eq.(16) gains

$$\dot{V} = s\dot{s}. \tag{17}$$

Taking the time derivative of Eq.(13) yields

$$\dot{s} = \dot{e} + \lambda e. \tag{18}$$

Substituting Eq.(18) and Eq.(1) into Eq.(17) yields

$$\begin{aligned} \dot{V} &= s(\dot{e} + \lambda e) \\ &= s(\dot{x}_d - \dot{x} + \lambda e) \\ &= s(\dot{x}_d - (a_0 x + a_1 u + a_2 w + \Phi) + \lambda e). \end{aligned} \tag{19}$$

Next, substituting the control law (i.e. Eq.14) into Eq.(19) acquires

$$\begin{aligned}\dot{V} &= s\left(\dot{x}_d - \left(\dot{x}_d + k_s\,|s|^{\varepsilon}\,\mathrm{sgn}(s) + a_2 w + a_0 x + \Phi + \lambda e\right)\right.\\ &\qquad \left. a_2 w + a_0 x + \lambda e\right)\\ &\le s(-k_s|s|^{\varepsilon}\mathrm{sgn}(s) + |\Phi|)\\ &\le |s|(-k_s|s|^{\varepsilon} + |\Phi|). \end{aligned} \tag{20}$$

According to Eq.(20), when $|s(t)| \le \left(\frac{\Phi}{k_s}\right)^{\frac{1}{\varepsilon}}$, we deduce that $\dot{V} < 0$. Hence, according to the Lyapunov theorem, the designed SMC is stable.

B. PERTURBATION ESTIMATION METHOD

The perturbation estimation method [22], [23] is briefly summarized in this section. We used this method to estimate the uncertainty parameters part and the external perturbation of the piezo-actuated stage system.

A generalized nonlinear system is expressed as follows

$$x^{(n)} = M\,(X) + \Delta M\,(X) + [G\,(X) + \Delta G\,(X)]\,u + q\,(t)\,, \tag{21}$$

where $X_i = \left[x_i, \dot{x}_i, \ldots, x_i^{(n_i-1)}\right]^T \in R^{n_i}, i = 1, 2, \ldots, m$ is the state sub-vector, $X = \left[X_1^T, X_2^T, \ldots, X_m^T\right] \in R^{\sum_{i=1}^{m} n_i}$ is the global state vector, the vector $x^{(n)} = \left[x_1^{(n_1)}, x_2^{(n_2)}, \ldots, x_m^{(n_i)}\right] \in R^m, i = 1, 2, \ldots, m$ is m independent coordinates.

The bounded perturbations of Eq.(21) can be summed up in the following vector form

$$\begin{aligned}\Phi\,(t) &= \Delta M(X) + \Delta G(X)u + q\,(t)\\ &= x^{(n)} - M\,(X) - G(X)u. \end{aligned} \tag{22}$$

The perturbation Φ can be estimated as

$$\Phi_{\mathrm{est}}\,(t) = x_{\mathrm{cal}}^{(n)} - M\,(X) - G(X)u\,(t-T)\,, \tag{23}$$

where T is the sampling interval, $x_{\mathrm{cal}}^{(n)}$ represents a calculated state vector that can be measured based on the following equation

$$x^n = \frac{x^{(n-1)}\,(t) - x^{(n-1)}\,(t-T)}{T}. \tag{24}$$

C. PROPOSED SMC METHOD DESIGN

According to the piezo-actuated stages system model (i.e. Eq.(11)), the piezo-actuated stages system with perturbation is expressed as follows

$$\dot{x}(t) = a_0 x(t) + a_1 u(t) + a_2 w(t) + \Phi(t). \tag{25}$$

The bounded perturbations can be written as

$$\begin{aligned}\Phi_{\mathrm{act}}(t) &= \Delta_0 x(t) + \Delta_1 u(t) + \Delta_2 w(t) + f(t)\\ &= \dot{x}(t) - a_0 x(t) - a_1 u(t) - a_2 w(t). \end{aligned} \tag{26}$$

where Φ_{act} is composed of the disturbance, the modeling uncertainty part etc, which can be estimated based on the perturbation estimation method as [22]

$$\Phi_{\mathrm{est}}(t) = \dot{x}(t) - a_0 x(t) - a_1 u(t-T) - a_2 w(t-T). \tag{27}$$

To design the controller, a new reaching law is proposed as follows

$$\dot{s} = -k_s\,|s|^{\varepsilon}\,\mathrm{sgn}(s) - \eta \mathrm{sgn}(s), \tag{28}$$

where ε is a positive constant $0 \le \varepsilon \le 1$, η is the switching gain.

Considering the perturbation of the system, the Eq.(28) becomes

$$\begin{aligned}\dot{s} &= -k_s\,|s|^{\varepsilon}\,\mathrm{sgn}\,(s) - \eta \mathrm{sgn}\,(s) + \Phi_{\mathrm{est}}\,(t) - \Phi_{\mathrm{act}}\,(t)\\ &= -k_s\,|s|^{\varepsilon}\,\mathrm{sgn}\,(s) - \eta \mathrm{sgn}\,(s) + \hat{\Phi}\,(t)\,, \end{aligned} \tag{29}$$

where $\hat{\Phi}\,(t)$ is the error between Φ_{est} and Φ_{act}.

In order to verify the proposed reaching law can guarantee the stability of the proposed control system, we use the same Lyapunov function as Eq.(16), and its first order derivative is same as Eq.(17). Subsequently, substituting Eq.(29) into Eq.(17) yields

$$\begin{aligned}\dot{V} &= s\left(-k_s\,|s|^{\varepsilon}\,\mathrm{sgn}\,(s) - \eta \mathrm{sgn}\,(s) + \hat{\Phi}\right)\\ &= -k_s s\,|s|^{\varepsilon}\,\mathrm{sgn}\,(s) - \eta\,|s| + \hat{\Phi} s\\ &\le -k_s\,|s|^{\varepsilon+1} - \eta\,|s| + \hat{\Phi}\,|s|\,. \end{aligned} \tag{30}$$

Considering Eq.(30), η is designed to satisfy the condition

$$\eta > \hat{\Phi} \Rightarrow \dot{V} < 0.$$

Because the proposed reaching law satisfies the Lyapunov stability conditions, the switching function can converge on the switching surface in limited time. Based on Eq.(28), the controller is designed as

$$\begin{aligned}u = \frac{1}{a_1}(\dot{x}_d + \lambda x_d - (\lambda + a_0)x) + k_s|s|^{\varepsilon}\mathrm{sgn}(s) + \eta\mathrm{sgn}(s)\\ - \frac{a_2}{a_1}w - \frac{1}{a_1}\Phi_{\mathrm{est}}. \end{aligned} \tag{31}$$

Next, substituting Eq.(27) into Eq.(31), the result is Eq.(32).

$$\begin{aligned}u\,(t) &= \frac{1}{a_1}(\dot{x}_d(t) + \lambda x_d(t) - (\lambda + a_0)x(t))\\ &\quad + k_s|s|^{\varepsilon}\mathrm{sgn}(s) + \eta\mathrm{sgn}(s) - \frac{a_2}{a_1}w(t)\\ &\quad - \frac{1}{a_1}\left(\dot{x}(t) - a_0 x(t) - a_1 u(t-T) - a_2 w(t-T)\right)\\ &= \frac{1}{a_1}(\dot{e}(t) + \lambda e(t)) - \frac{a_2}{a_1}(w(t) - w(t-T))\\ &\quad + u(t-T) + k_s|s|^{\varepsilon}\mathrm{sgn}(s) + \eta\mathrm{sgn}(s). \end{aligned} \tag{32}$$

Proof: To prove the stability of the system, substituting Eq.(32) into Eq.(17) yields

$$\begin{aligned}\dot{V} &= s\,(\dot{e}\,(t) + \lambda e\,(t))\\ &= s\,(\dot{x}_d\,(t) - \dot{x}\,(t) + \lambda e\,(t)) \end{aligned}$$

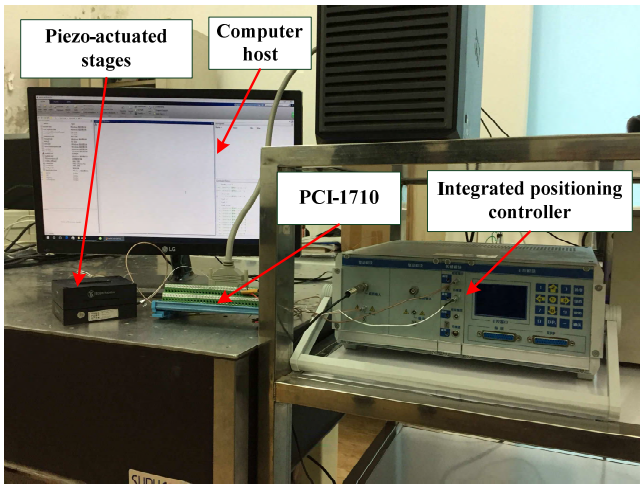

FIGURE 3. Experimental setup of piezo-actuated stages.

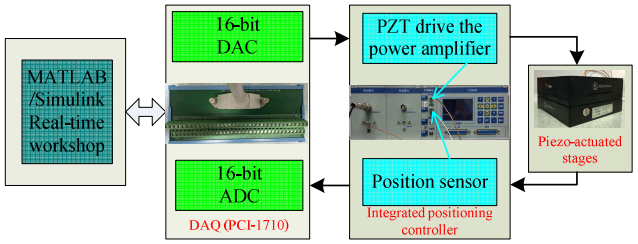

FIGURE 4. Structure diagram of experimental setup.

$$
\begin{aligned}
&= s\left(\dot{x}_d(t) - a_0 x(t) - a_2 w(t) + \lambda e(t) - \right. \\
&\quad a_1\left(\frac{1}{a_1}(\dot{e}(t) + \lambda e(t)) - \frac{a_2}{a_1}(w(t) - w(t-T))\right. \\
&\qquad \left.\left. + u(t-T) + k_s|s|^{\varepsilon}\mathrm{sgn}(s) + \eta \mathrm{sgn}(s)\right)\right) \\
&\quad -(\Phi_{\mathrm{est}} - \hat{\Phi})s \\
&\le -k_s|s|^{\varepsilon}\mathrm{sgn}(s)s - \eta \mathrm{sgn}(s)s + \hat{\Phi}|s| \\
&\le -k_s|s|^{\varepsilon+1} - \eta|s| + \hat{\Phi}|s| \qquad (33)
\end{aligned}
$$

According to Eq.(33), the switching gain η should satisfy the condition as follow

$$\eta > \hat{\Phi} \Rightarrow \dot{V} < 0,$$

Hence, the proposed controller satisfies the Lyapunov stability criterion in this study.

In addition, with increase in the perturbation of the system, the switching gain k_s becomes larger and the system generates the chattering. To decrease the chattering of the signum function, the saturation function Eq.(34) is adopted to replace the signum function.

$$\mathrm{sat}(s) = \begin{cases} 1 & s > \Delta \\ ks & |s| < \Delta, k = 1/\Delta \\ -1 & s < -\Delta, \end{cases} \qquad (34)$$

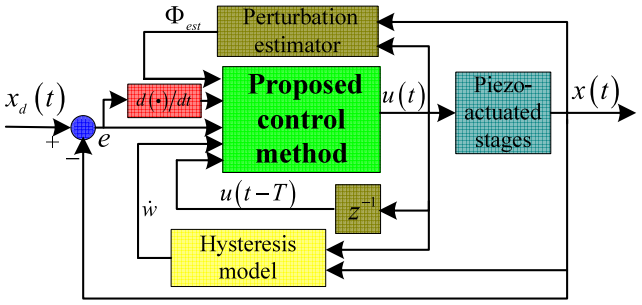

FIGURE 5. Block diagram of the proposed controller.

TABLE 2. Parameters of the controller.

Controller	Parameters	Value
CSMC	k_s	1
	ε	0.9
	λ	2300
Propored controller	k_s	0.3
	ε	0.8
	λ	1900
	η	3.6

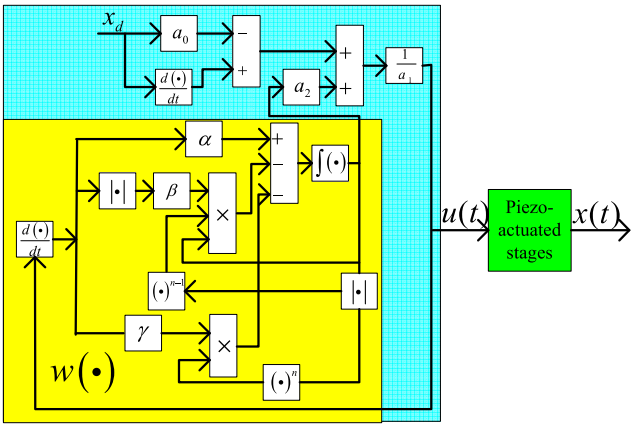

FIGURE 6. Block diagram of feed-forward controller.

TABLE 3. Control results of the triangular signal motion tracking with various frequencies.

Frequency		Feed-forward	CSMC	Proposed controller
0.1Hz	MAX error(μm)	1.0607	0.9083	0.3556
	Percentage(%)	2.95	2.52	0.98
	RMS(μm)	0.3950	0.2973	0.0194
1Hz	MAX error(μm)	1.001	0.9862	0.4243
	Percentage(%)	2.78	2.74	1.18
	RMS(μm)	0.4341	0.4652	0.0695
10Hz	MAX error(μm)	2.0325	1.7538	0.7064
	Percentage(%)	5.64	4.87	1.96
	RMS(μm)	0.6838	0.6677	0.1327

where Δ is the thickness of the boundary layer, which is a positive constant. Subsequently, the effect of the controller based on the above method is proved by the experimental setup of the piezo-actuated stages in section IV.

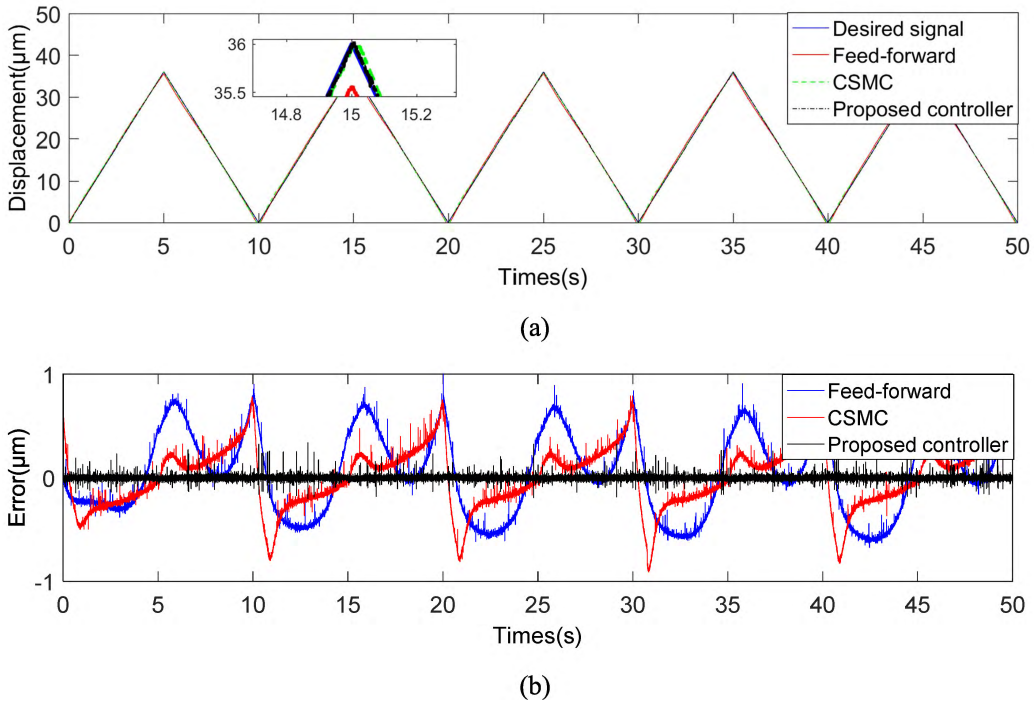

FIGURE 7. Results of triangular signal motion tracking with amplitude of 36μm and frequency of 0.1Hz. (a) Tracking result and desired signal. (b) Tracking error.

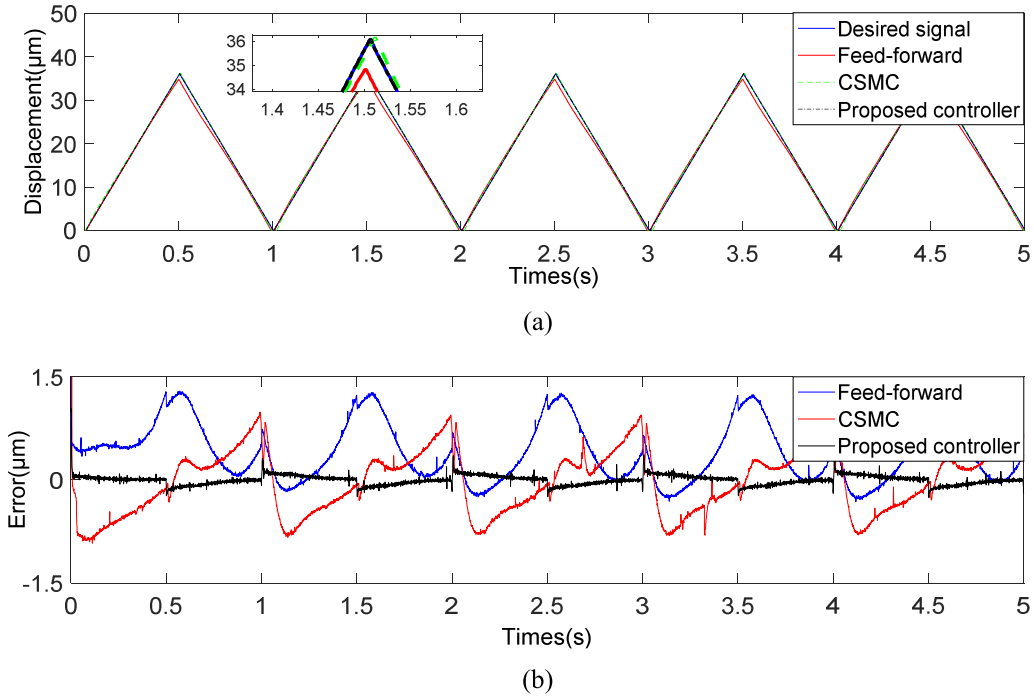

FIGURE 8. Results of triangular signal motion tracking with amplitude of 36μm and frequency of 1Hz. (a) Tracking result and desired signal. (b) Tracking error.

IV. EXPERIMENTAL RESULTS

A. EXPERIMENTAL SETUP AND CONTROL PARAMETER DESIGN

To demonstrate the effectiveness of the proposed controller, the experiment is conducted on a commercial piezo-actuated stages(MPT-2MRL102A, Boshi Robotics). The experimental setup is shown in Fig. 3. The integrated positioning controller (PPC-2CR0150, Boshi Robotics) is composed of an electric resistance strain gauge position sensor and a high-voltage amplifier. The electric resistance strain gauge

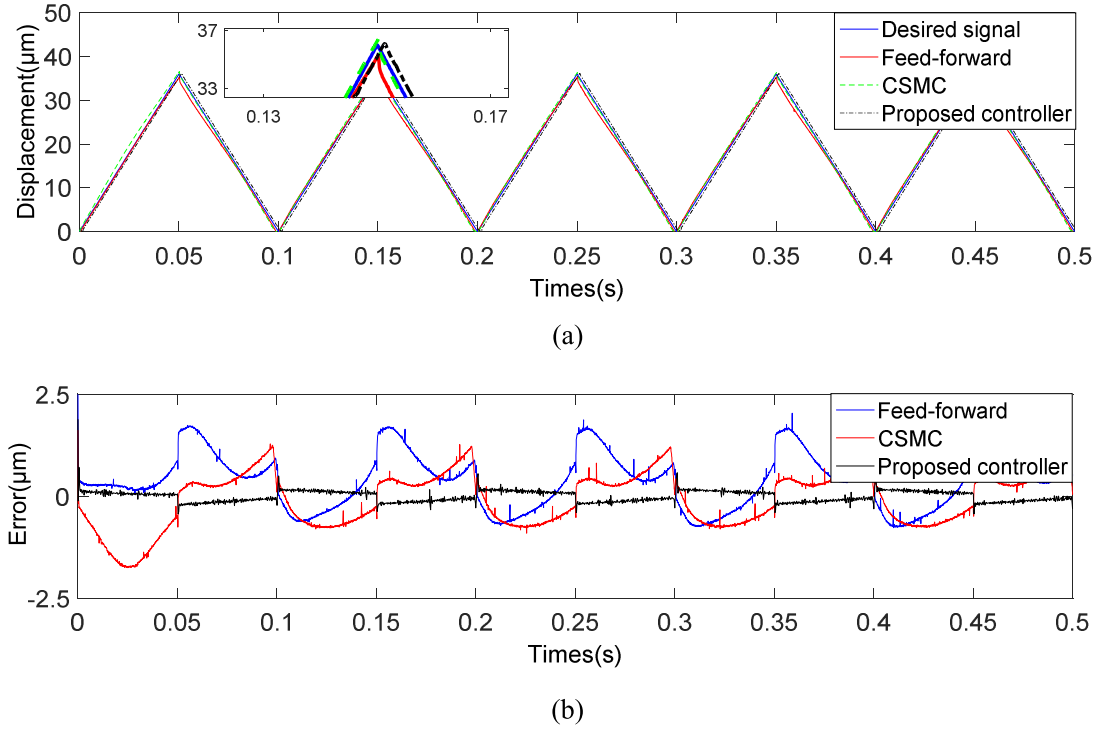

FIGURE 9. Results of triangular signal motion tracking with amplitude of 36μm and frequency of 10Hz. (a) Tracking result and desired signal. (b) Tracking error.

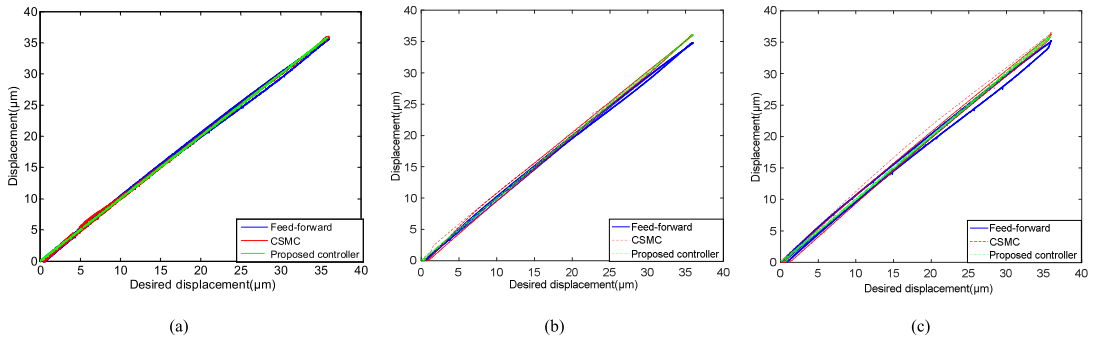

FIGURE 10. Hysteresis plots of piezo-actuated stages based on control strategies with different frequencies. (a) 0.1Hz. (b) 1Hz. (c) 10Hz.

position sensor is employed to measure the actual output displacement of the piezo-actuated stage. The high-voltage amplifier amplifies the input voltage signal of the piezo-actuated stage from 0-10 V to 0-150 V. A host computer installed with the MATLAB/Simulink software is used to implement the control strategies and the operation state estimation. A data acquisition card (PCI-1710, Advantech) is used as the digital-analog (D/A) and analog-digital (A/D) converter between the host computer and the piezo-actuated stage. The experiments are conducted with a sample frequency of 10kHz. The structure diagram of the experimental setup is shown in Fig. 4. The block diagram of the proposed control method is shown in Fig. 5.

In this study, we adopted the feed-forward controller and the CSMC method as a comparison to verify the effectiveness of the proposed controller. The block diagram of the feed-forward controller based on the inverse Bouc-Wen model is shown in Fig. 6. The inverse Bouc-Wen model can be derived using the mathematical method [13], [15]. Because the inverse model is obtained using the mathematical method, the parameters of the feed-forward controller are same as the identified Bouc-Wen model based on the bat-inspired algorithm. Another comparison method is the CSMC (i.e. Eq.(14)) with the switching gain k_s, ε, and the control gain λ. The parameters of the proposed controller contain the switching gain η in contrast to the CSMC method.

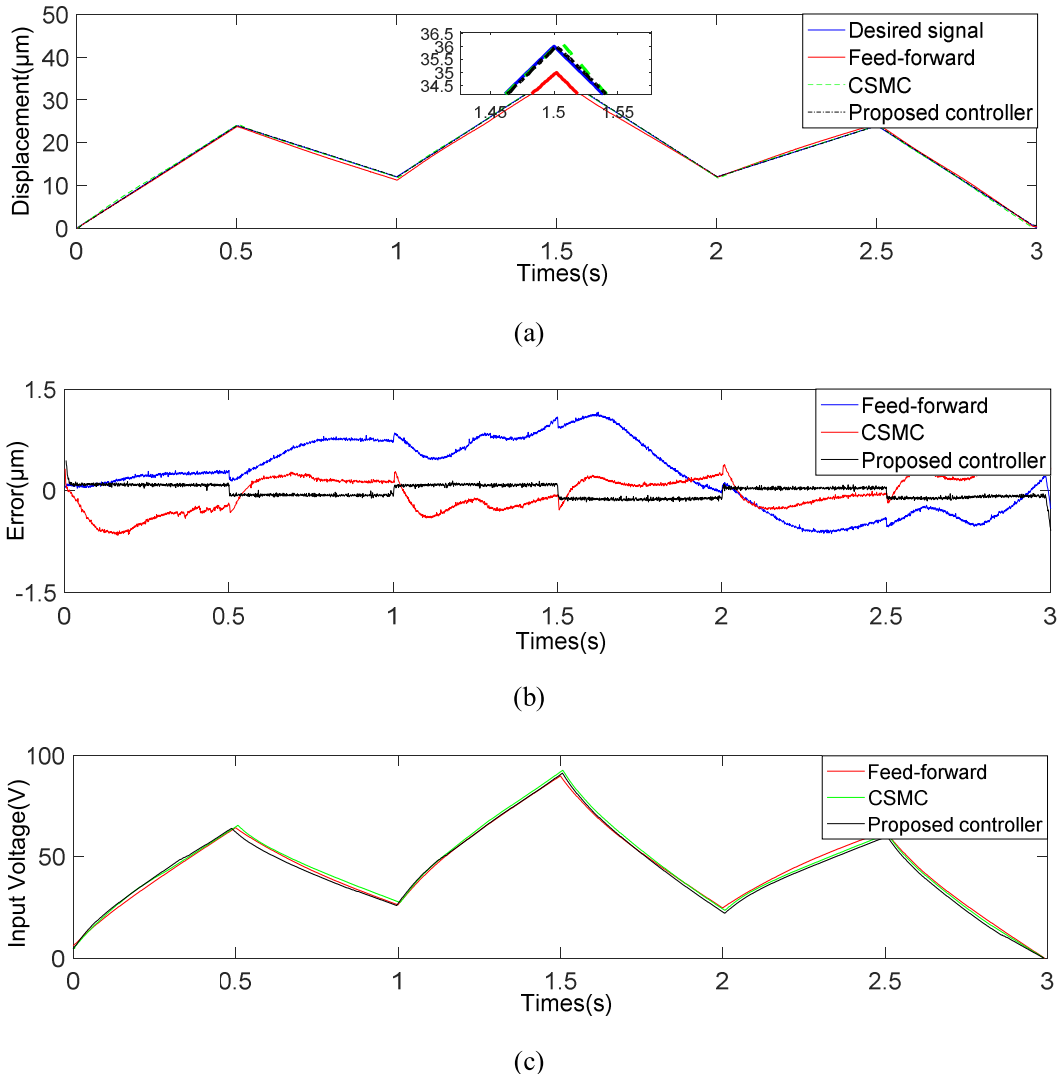

FIGURE 11. Results of the multi-amplitude triangular signal position tracking. (a) Tracking result and desired signal. (b) Tracking error. (c) Control input voltages.

In addition, the control parameters of the CSMC method are set using the trial-and-error method. It is well known that the control precision of the SMC method is improved with the increase of the switching gain and the control gain [34]. However, the large gains can cause the instability of the system. To indicate the performance of the proposed controller, the switching gain k_s, ε, and the control gain λ of the proposed control method are both less compared with the CSMC method while maintaining the system stability. The switching gain η of the proposed control method is set as 3.6 using the trial-and-error method. The parameters of the CSMC and the proposed control methods are listed in Table 2.

B. TRIANGULAR SIGNAL MOTION TRACKING

To demonstrate the effectiveness of the proposed control method, the triangular signals with frequencies of 0.1Hz, 1Hz, and 10Hz are tracked using the feed-forward control, CSMC and proposed control methods, respectively. The results of the tracking experiment under three different frequencies are shown in Fig. 7(a), Fig. 8(a), and Fig. 9(a), respectively. It is evident that the output displacement of the piezo-actuated stage based on the proposed control method is consistent with the desired signal in a very excellent way. The tracking errors are shown in Fig. 7(b), Fig. 8(b), and Fig. 9(b), respectively. The MAX tracking error and the root mean square (RMS) error are shown in Table 3. When the frequency of the desired signal is 0.1Hz, the MAX tracking error and the RMS error of the proposed control method are 0.3556 μm and 0.0194 μm, respectively. Compared with the feed-forward control, the proposed control method reduces the MAX tracking error and the RMS error by 66.5% and 95.1%; compared with the CSMC method, the proposed control method attenuates the MAX tracking error and the RMS

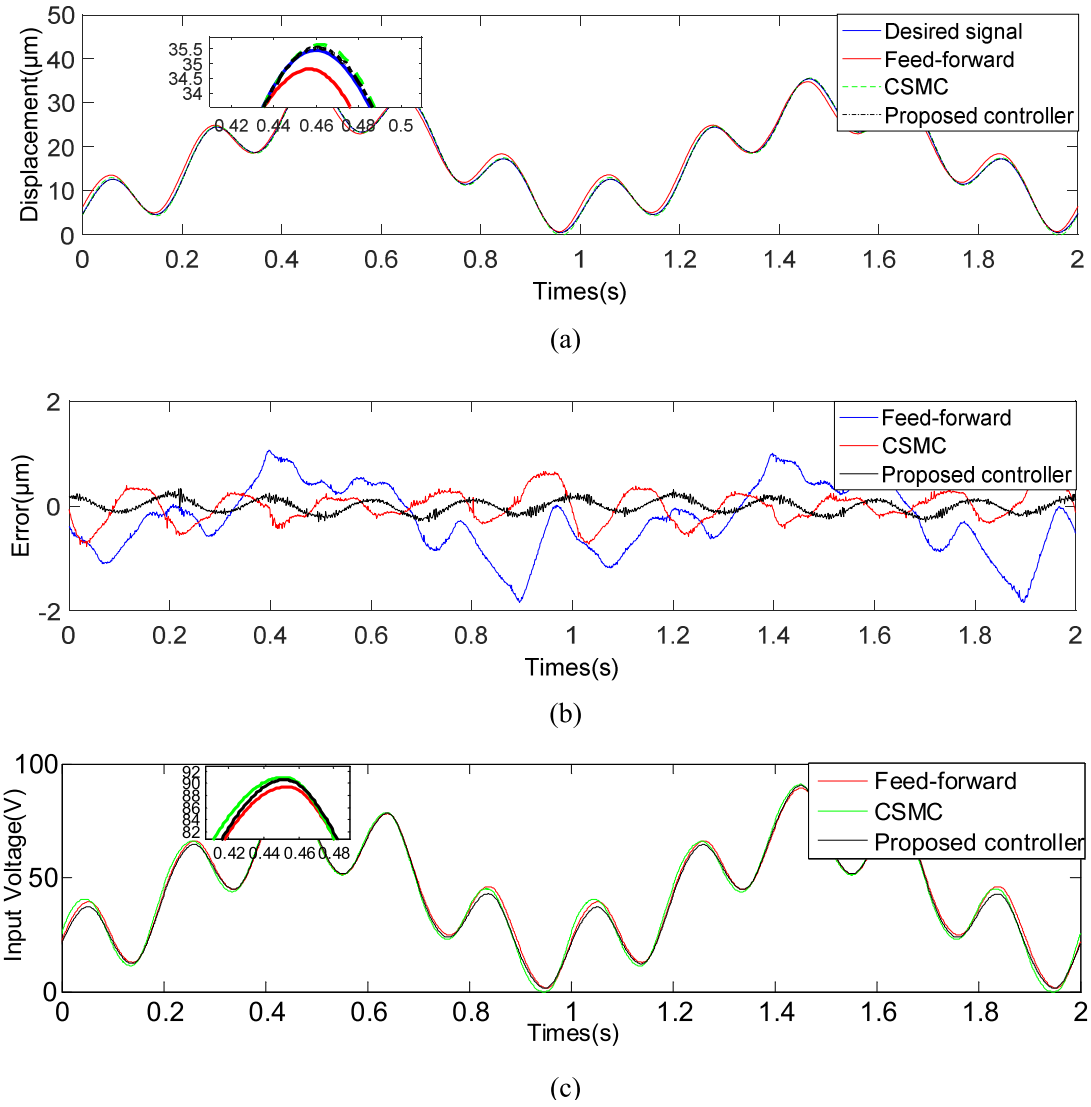

FIGURE 12. Results of complex harmonic signal motion tracking. (a) Tracking result and desired signal. (b) Tracking error. (c) Control input voltages.

error by 60.8% and 93.5%, respectively. When the frequency of the desired signal is 1Hz, the MAX tracking error and the RMS error of the proposed control method are 0.4243 μm and 0.0695 μm, respectively. Compared with the feed-forward control, the proposed control method reduces the MAX tracking error and the RMS error by 57.6% and 83.9%; compared with the CSMC method, the proposed control method attenuates the MAX tracking error and the RMS error by 56.9% and 85.1%, respectively. When the frequency of the desired signal is 10Hz, the proposed control method provides the MAX tracking error of 0.7064 μm and the RMS error of 0.1327 μm, which decreases by 65.2% and 80.6% in comparison with the feed-forward control; compared with the CSMC method, the MAX tracking error and the RMS error of the proposed control method decreases by 59.7% and 78.2%, respectively. In addition, the hysteresis plots of the piezo-actuated stage based on the control strategies are shown in Fig. 9. It is evident that the hysteresis nonlinearity of the piezo-actuated stage can be suppressed in various degrees using these three control methods. Nonetheless, in the subdued hysteresis curves based on the feed-forward controller and the CSMC method the backlash evidently still exist as shown in Fig. 10, the hysteresis nonlinearity of the piezo-actuated stage based on the proposed control method is considerably suppressed.

To further certify the performance of the proposed controller, we have compared the experimental results of the proposed controller with that of a fast non-singular terminal SMC method [35]. The robust and fast non-singular terminal SMC produces the MAX tracking error rate of 2.5% and RMS error rate of 0.92% for a triangular signals with

TABLE 4. Control results of the multi-amplitude triangular signal motion tracking.

Controller	MAX error(μm)	Percentage(%)	RMS error (μm)
Feed-forward	1.4367	3.99	0.5028
CSMC	0.7409	2.06	0.2709
Proposed controller	0.5918	1.64	0.0913

frequencies of 10Hz. In particular, the proposed control method can alleviate the MAX tracking error and RMS error by 21.6% and 59.8%, respectively. Hence, the proposed control method outperforms the other robust control method.

C. MULTI-AMPLITUDE TRIANGULAR SIGNAL MOTION TRACKING

The multi-amplitude triangular signal with the MAX amplitude of 36 μm is used as the desired signal to prove the effectiveness of the proposed controller on the piezo-actuated stages. The position tracking results of the multi-amplitude triangular signal based on the three different controllers are shown in Fig. 11(a). The tracking errors are shown in Fig. 11(b). The input voltages of the piezo-actuated stage based on the three controllers are depicted in Fig. 11(c). The MAX tracking errors and the RMS errors are described in Table 4. We can observe from Table 4 that the proposed control method reduces the MAX tracking error and the RMS error by 58.8% and 81.8%, respectively, in comparison with the feed-forward control. Moreover, in contrast with the CMSC method, the proposed control method reduces the MAX tracking error and the RMS error by 20.1% and 66.3%, respectively. It is evident that the proposed controller can effectively eliminate the hysteresis nonlinearity of the piezo-actuated stages and has the best performance in terms of the multi-amplitude triangular signal motion tracking.

D. COMPLEX HARMONIC SIGNAL MOTION TRACKING

To further demonstrate the performance of the proposed controller, $y_d = 12\sin(2\pi t - 0.5\pi) + 6\sin(10\pi t) + 18$ is used as the desired signal for the experiment. The tracking results of the complex harmonic signal based on the three different controllers are shown in Fig. 12(a). The tracking errors are shown in Fig. 12(b). The output voltage signals of the three controllers are described in Fig. 12(c). In Table 5, the comparative tracking results of the three controllers are listed. Compared with the feed-forward control, the proposed control method mitigates the MAX tracking error and the RMS error by 81.65% and 80.6%, respectively; compared with the CMSC method, the MAX tracking error and the RMS error of the proposed control method decreases by 55.3% and 56.9%, respectively. It is evident that the proposed control method outperforms both feed-forward control and the CSMC method. In addition, compared with the model predictive discrete-time SMC method [36] that achieved the

TABLE 5. Control results of complex harmonic signal motion tracking.

Controller	MAX error(μm)	Percentage(%)	RMS error (μm)
Feed-forward	1.8366	5.10	0.6528
CSMC	0.7669	2.13	0.2932
Proposed controller	0.3371	0.94	0.1263

MAX tracking error rate of 1.20% and the RMS error rate of 0.44% for a sinusoidal signal with frequency of 2Hz, the proposed control method (for a complex harmonic signal of 1Hz and 5Hz) can decrease the MAX and RMS error by 21.7% and 20.5%, respectively. After a series of comparative experiments, the performance of the proposed control method is amply demonstrated.

V. CONCLUSION

In this study, the hysteresis nonlinearity of the piezo-actuated stages is described using the Bouc-Wen model, which is identified by the bat-inspired algorithm. The experimental results indicate that the MAX error of the model is only 0.9651 μm. Subsequently, a SMC method based on the Bouc-Wen model is proposed for eliminating the hysteresis nonlinearity effect in the piezo-actuated stages. The stability of the proposed control system is verified using the Lyapunov theory. The effectiveness of the proposed control method is verified by conducting a series of experimental studies. The experimental results validate that the proposed control method can effectively suppress the hysteresis nonlinearity effect to achieve high precision tracking control of the piezo-actuated stages. Moreover, in comparison with the feed-forward control and the CSMC method, the proposed control method can improve the RMS error by more than 50% under different reference signals. The proposed control method exhibits a superior performance in comparison with the feed-forward control and the CSMC method. In the future, the proposed control method can dispense with the inverse hysteresis model and can be easily applied to other micropositioning stages.

REFERENCES

[1] S. T. Ho and S. J. Jan, "A piezoelectric motor for precision positioning applications," *Precis. Eng.*, vol. 43, pp. 285–293, Jan. 2016.

[2] H. Li, Y. Li, T. Cheng, X. Lu, H. Zhao, and H. Gao, "A symmetrical hybrid driving waveform for a linear piezoelectric stick-slip actuator," *IEEE Access*, vol. 5, pp. 16885–16894, Aug. 2017.

[3] K. K. Leang, Q. Zou, and S. Devasia, "Feedforward control of piezoactuators in atomic force microscope systems," *IEEE Control Syst.*, vol. 29, no. 1, pp. 70–82, Feb. 2009.

[4] R. Xu and M. Zhou, "A self-adaption compensation control for hysteresis nonlinearity in piezo-actuated stages based on Pi-sigma fuzzy neural network," *Smart. Mater. Struct.*, vol. 27, no. 4, pp. 045002-1–045002-13. Feb. 2018.

[5] I. Ahmad, "Two degree-of-freedom robust digital controller design with Bouc-Wen hysteresis compensator for piezoelectric positioning stage," *IEEE Access*, vol. 6, pp. 17275–17283, Mar. 2018, doi: 10.1109/ACCESS.2018.2815924.

[6] R. Dong, Y. Tan, Y. Xie, and K. Janschek, "Recursive identification of micropositioning stage based on sandwich model with hysteresis," *IEEE Trans. Control. Syst. Technol.*, vol. 25, no. 1, pp. 317–325, Jan. 2017.

[7] X. Y. Zhang *et al.*, "Fuzzy approximator based adaptive dynamic surface control for unknown time delay nonlinear systems with input asymmetric hysteresis nonlinearities," *IEEE Trans. Syst., Man, Cybern., Syst.*, vol. 47, no. 8, pp. 2218–2232, Aug. 2017.
[8] H. Hu and R. B. Mrad, "On the classical Preisach model for hysteresis in piezoceramic actuators," *Mechatron.*, vol. 13, no. 2, pp. 85–94, Mar. 2003.
[9] M. Edardar, X. Tan, and H. K. Khalil, "Sliding-mode tracking control of piezo-actuated nanopositioners," in *Proc. Amer. Control Conf.*, Montreal, QC, Canada, Jun. 2012, pp. 3825–3830.
[10] R. Xu and M. Zhou, "Elman neural network-based identification of Krasnosel'skii–Pokrovskii model for magnetic shape memory alloys actuator," *IEEE Trans. Magn.*, vol. 11, no. 5, pp. 2002004-1–2002004-4, Nov. 2017.
[11] D. Habineza, M. Rakotondrabe, and Y. Le Gorrec, "Bouc–Wen modeling and feedforward control of multivariable hysteresis in piezoelectric systems: Application to a 3-dof piezotube scanner," *IEEE Trans. Control. Syst. Technol.*, vol. 23, no. 5, pp. 1797–1806, Sep. 2015.
[12] Y. Liu, J. Shan, U. Gabbert, and N. Qi, "Hysteresis and creep modeling and compensation for a piezoelectric actuator using a fractional-order Maxwell resistive capacitor approach," *Smart. Mater. Struct.*, vol. 22, no. 11, pp. 115020-1–115020-12, Oct. 2013.
[13] M. Rakotondrabe, "Bouc–Wen modeling and inverse multiplicative structure to compensate hysteresis nonlinearity in piezoelectric actuators," *IEEE Trans. Autom. Sci. Eng.*, vol. 8, no. 2, pp. 428–431, Apr. 2011.
[14] P. Ge and M. Jouaneh, "Tracking control of a piezoceramic actuator," *IEEE Trans. Control Syst. Technol.*, vol. 4, no. 3, pp. 209–216, Mar. 1996.
[15] Z. Wang, Z. Zhang, and J. Mao, "Precision tracking control of piezoelectric actuator based on Bouc-Wen hysteresis compensator," *Electron. Lett.*, vol. 48, no. 23, pp. 1459–1460, Nov. 2012.
[16] A. H. El-Shaer, M. Al Janaideh, P. Krejčí, and M. Tomizuka, "Robust performance enhancement using disturbance observers for hysteresis compensation based on generalized Prandtl–Ishlinskii model," *J. Dyn. Syst. Meas. Control*, vol. 135, no. 5, pp. 051008-1–051008-13, May 2013.
[17] Y. Guo, J. Mao, and K. Zhou, "Rate-dependent modeling and control of GMA based on Hammerstein model with Preisach operator," in *Proc. Int. Conf. Mechatronics Autom. (ICMA)*, Aug. 2012, pp. 343–347.
[18] Q. Xu, "Adaptive discrete-time sliding mode impedance control of a piezoelectric microgripper," *IEEE Trans. Robot.*, vol. 29, no. 3, pp. 663–673, Jun. 2013.
[19] M. Edardar, X. Tan, and H. K. Khalil, "Design and analysis of sliding mode controller under approximate hysteresis compensation," *IEEE Trans. Control Syst. Technol.*, vol. 23, no. 2, pp. 598–608, Mar. 2015.
[20] A. M. Shotorbani, A. Ajami, S. G. Zadeh, M. P. Aghababa, and B. Mahboubi, "Robust terminal sliding mode power flow controller using unified power flow controller with adaptive observer and local measurement," *IET Generat., Transmiss. Distribut.*, vol. 8, no. 10, pp. 1712–1723, Oct. 2014.
[21] M. Jin, J. Lee, and K. K. Ahn, "Continuous nonsingular terminal sliding-mode control of shape memory alloy actuators using time delay estimation," *IEEE/ASME Trans. Mechatronics*, vol. 20, no. 2, pp. 899–909, Apr. 2015.
[22] H. Elmali and N. Olgac, "Implementation of sliding mode control with perturbation estimation (SMCPE)," *IEEE Trans. Control. Syst. Technol.*, vol. 4, no. 1, pp. 79–85, Jan. 1996.
[23] N. I. Kim, C. W. Lee, and P. H. Chang, "Sliding mode control with perturbation estimation: application to motion control of parallel manipulator," *Control. Eng. Pract.*, vol. 6, no. 11, pp. 1321–1330, Nov. 1998.
[24] H. Komurcugil, S. Ozdemir, and I. Sefa, "Sliding-mode control for single-phase grid-connected L*CL*-filtered VSI with double-band hysteresis scheme," *IEEE Trans. Ind. Electron.*, vol. 63, no. 2, pp. 864–873, Feb. 2016.
[25] R. Xu and M. Zhou, "Sliding mode control with sigmoid function for the motion tracking control of the Piezo-actuated stages," *Electron. Lett.*, vol. 53, no. 2, pp. 75–77, Jan. 2017.
[26] Q. Xu, "Continuous integral terminal third-order sliding mode motion control for piezoelectric nanopositioning system," *IEEE/ASME. Trans. Mechatron.*, vol. 22, no. 4, pp. 1828–1838, Aug. 2017.
[27] R. Bouc, "Forced vibrations of mechanical systems with hysteresis," in *Proc. 4th Conf. Nonlinear Oscillations*, Prague, Czechoslovakia, 1967, pp. 32–39.
[28] Y.-K. Wen, "Method for random vibration of hysteretic systems," *J. Eng. Mech. Division*, vol. 102, no. 2, pp. 249–263, 1976.
[29] M. Ye and X. Wang, "Parameter estimation of the Bouc–Wen hysteresis model using particle swarm optimization," *Smart. Mater. Struct.*, vol. 16, no. 6, pp. 2341–2349, Oct. 2017.
[30] G. Wang, G. Chen, and F. Bai, "Modeling and identification of asymmetric Bouc–Wen hysteresis for piezoelectric actuator via a novel differential evolution algorithm," *Sens. Actuators A, Phys.*, vol. 235, pp. 105–118, Nov. 2015.
[31] X. S. Yang, "A new metaheuristic bat-inspired algorithm," in *Nature Inspired Cooperative Strategies for Optimization*. Berlin, Germany: Springer, 2010, pp. 65–74.
[32] T. C. Bora, L. S. Coelho, and L. Lebensztajn, "Bat-inspired optimization approach for the brushless DC wheel motor problem," *IEEE Trans. Magn.*, vol. 48, no. 2, pp. 947–950, Feb. 2012.
[33] P. W. Tsai, J. S. Pan, B. Y. Liao, M. J. Tsai, and V. Istanda, "Bat algorithm inspired algorithm for solving numerical optimization problems," *Appl. Mech. Mater.*, vol. 148, no. 1, pp. 134–137, Dec. 2011.
[34] Q. Xu, "Precision motion control of Piezoelectric nanopositioning stage with chattering-free adaptive sliding mode control," *IEEE Trans. Autom. Sci. Eng.*, vol. 14, no. 1, pp. 238–248, Jan. 2017.
[35] A. Al-Ghanimi, J. Zheng, and Z. Man, "Robust and fast non-singular terminal sliding mode control for piezoelectric actuators," *IET. Control Theory. Appl.*, vol. 9, no. 18, pp. 2678–2687, Dec. 2015.
[36] Q. Xu and Y. Li, "Model predictive discrete-time sliding mode control of a nanopositioning piezostage without modeling hysteresis," *IEEE Trans. Control Syst. Technol.*, vol. 20, no. 4, pp. 983–994, Jul. 2012.

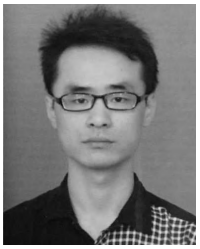

RUI XU was born in Dongying, China. He received the B.S. degree in automation from the Changchun University of Technology in 2014. He is currently pursuing the Ph.D. degree in control theory and control engineering with the Department of Control Science and Engineering, Jilin University, Changchun, China.

His research interests include micro-/nano-drive and control technology and nonlinear control theory.

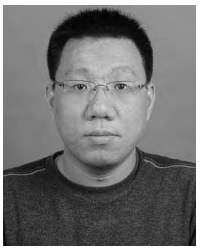

XIUYU ZHANG (M'17) was born in Jilin City, China. He received the B.S. and M.S. degrees from Northeast Dianli University, Jilin City, in 2003 and 2006, respectively, and the Ph.D. degree from the Beijing University of Aeronautics and Astronautics, Beijing, China, in 2012.

He is currently a Professor with the School of Automation Engineering, Northeast Dianli University. His research interests include robust and adaptive control for nonlinear systems with smart material-based actuators.

HONGYAN GUO (M'17) received the Ph.D. degree from Jilin University, Changchun, China, in 2010. She joined Jilin University in 2011, where she was an Associate Professor with the Department of Control Science and Engineering in 2014. In 2017, She was a Visiting Scholar with Cranfield University, U.K.

Her current research interests include path tracking and stability control of autonomous vehicles and vehicle states estimation.

MIAOLEI ZHOU (M'14) was born in 1976. He received the B.S. and M.S. degrees in industrial electric automation from the Jilin Institute of Technology, China, in 1997 and 2000, respectively, and the Ph.D. degree in control theory and control engineering from Jilin University, China, in 2004. From 2006 to 2008, he was a Post-Doctoral Researcher with Tokyo University, Japan.

In 2000, he joined the Department of Control Science and Engineering, Jilin University, where he became an Associate Professor in 2009 and a Professor in 2014. He has supervised over 20 research projects, including the National Natural Science Funds of China and the National High Technology Research and Development Program. He has authored over 70 papers. His research interests include micro-/nano-drive and control technology, nonlinear control theory, and navigation and control of robot. He is an Editorial Board Member of the *Scientific Journal of Control Engineering*.